Journal of Applied Science and Engineering, Vol. 21, No. 4, pp. 603–608 (2018) *DOI: 10.6180/jase.201812_21(4).0013*

Ground Target Localization Algorithm Based on Unmanned Aerial Vehicle Image Analysis

Rui Huang* and Binwu Ji

Guilin University of Aerospace Technology, Guilin 541004, P.R. China

Abstract

Locating ground targets in unmanned aerial vehicle images is a key problem in computer vision and UAV applications. In this paper, we propose a novel ground target localization algorithm based on the image process technique. The main idea of this paper is to utilize scale-invariant feature transform (SIFT) feature descriptor to tackle the proposed problem. SIFT feature descriptor can extract feature points which are invariant to scaling, orientation, affine transforms and illumination changes. Firstly, SIFT descriptors are matched from UAV images and coarse positioning result, and location points are extracted from UAV images. Secondly, coordinates in coarse positioning results are gained from remote sensing images using the radiation transformation model, and the final ground target localization results are obtained from the coordinate transformation relation. Experimental results demonstrate that the proposed algorithm can detect and locate ground target in UAV images with high accuracy.

***Key Words*:** Ground Target Localization, Unmanned Aerial Vehicle, Image Analysis, SIFT Feature

1. Introduction

An unmanned aerial vehicle (UAV), also named as an unmanned aircraft system (UAS), refers to an aircraft without a human pilot. The flight of UAVs may operate with different degrees of autonomy, that is, 1) remote control by human pilots, 2) completely autonomous by computers [1,2]. Different from aircraft controlled by humans, UAVs are suitable to be used in dull, dirty or dangerous environments. Due to the characteristics of low cost, no casualties' risk, strong survival ability, UAV performs better than ordinary reconnaissance and satellite systems [3,4]. Furthermore, the UAV aerial images has been widely utilized in dangerous areas investigating, real-time detection of battlefield, marine environmental monitoring, natural disaster detection, and so on. Hence, UAV image analysis has attracted more and more attention from researchers [5–7]. Some typical unmanned aerial vehicles are shown in Figure 1.

In Figures 1(a), 1(b) and 1(c), it means the Penguin B fixed-wing UAVs from UAV factory equipped with Cloud-Cap Piccolo autopilot system, X8 fixed-wing UAVs equipped with Ardupilot autopilot systems, and Microdrone MD4-1000 equipped with Ardupilot autopilot systems respectively.

This paper demonstrates on the problem of locate the position of ground targets by unmanned aerial vehicle image analysis, which is a key issue in UAV image process. For the best of our knowledge, target localization has been studied in recent years.

Feng et al. proposed a fast efficient power allocation algorithm used to cognitive distributed multiple radar systems, which highly relied on an alternating global search algorithm. Furthermore, this work aimed to minimize the non-convex CRLB of target location detection [8]. Chu et al. proposed an approach to calculate the error

(a) (b) (c)

Figure 1. Some typical unmanned aerial vehicles.

*Corresponding author. E-mail: taooyang@sina.com

signal delay discrimination using characteristic parameters, and the approach of Taylor series expansion location algorithm is presented as well [9]. Baghaee et al. studied the influence of environmental variations, (e.g. temperature, power supply fluctuations, magnetic noise, sensor sensitivity, and so on) on the target localization [10]. Einemo et al. tackled the issue of locating a target using multiple-input multiple-output radar with widely separated antennas. In particular, a quadratically constrained quadratic program for target localization is developed by linearizing the bistatic range measurements [11]. Vander et al. proposed a novel algorithm to locate a static target exploiting mobile robots installed with bearing sensors [12]. Matriche et al. proposed a novel approach to detect and locate buried metallic object in ElectroMagnetic Induction data with the kernel change detection algorithm. In particular, the goal of the given algorithm is to compute a decision index for each EMI measurement in hypotheses space [13]. Jang et al. proposed a location adaptive least square localization which deletes the weakness of the LS localization, and LA-LS algorithm can determine the receivers that produce abnormally large measurement errors with a proposed probabilistic measure [14]. Apart from the above works, other technologies have also been used in target localization, such as pseudogradient algorithm [15], false localization rate estimation using modified target-decoy [16], and deformable mesh registration [17].

The rest of the paper is organized as follows. We explain the SIFT feature descriptor in section 2. In section 3, we propose a novel ground target localization algorithm using the SIFT feature. Section 4 designs and implements a series of experiments to prove the effectiveness of our method. Section 5 concludes the whole paper.

2. Overview of SIFT Feature Descriptor

SIFT [18] feature descriptor is able to extract features which are invariant to scale, orientation, affine transforms and illumination changes. SIFT feature vector is represented as follows.

$$V(f_i)=\left(\begin{bmatrix} v_1(f_i) \\ \cdots \\ v_{n_i}(f_i) \end{bmatrix}, \begin{bmatrix} l_1(f_i) \\ \cdots \\ l_{n_i}(f_i) \end{bmatrix}\right) \tag{1}$$

where $v_1(f_i)$ refers to the feature vector of f_i. Moreover, $l_1(f_i)$ represents the location in image. Particularly, distance between $V(f_1)$ and $V(f_2)$ cannot be computed using the Euclidean distance directly.

In order to gain local descriptors, the derivatives d_{x1} and d_{x2} of the image region $R(x)$ are computed by the following equations.

$$d_{x1}(x_1,x_2)=R(x_1,x_2+1)-R(x_1,x_2-1) \tag{2}$$

$$d_{x2}(x_1,x_2)=R(x_1+1,x_2)-R(x_1-1,x_2) \tag{3}$$

Next, given an image region, magnitude (denoted as $M(\cdot)$) and orientation (denoted as $O(\cdot)$) are calculated as follows.

$$M(x_1,x_2)=\sqrt{d_{x1}(x_1,x_2)^2+d_{x2}(x_1,x_2)^2} \tag{4}$$

$$O(x_1,x_2)=\tan^{-1}\left(\frac{d_{x2}(x_1,x_2)}{d_{x1}(x_1,x_2)}\right) \tag{5}$$

The scale space of an image is represented as $L(x, y, \sigma)$, which is generated from the convolution of Gaussian $G(x, y, \sigma)$ [20], and the following equation is satisfied:

$$L(x,y,\sigma)=G(x,y,\sigma)\times I(x,y) \tag{6}$$

where $I(x, y)$ is the UAV image.

The scale space extrema is defined as $D(x, y, \sigma)$, which is computed as follows [20].

$$\begin{aligned} D(x,y,\sigma)&=(G(x,y,k\sigma)-G(x,y,\sigma))\cdot I(x,y) \\ &=L(x,y,k\sigma)-L(x,y,\sigma) \end{aligned} \tag{7}$$

where k is the constant multiplicative factor.

3. The Proposed Ground Target Localization Algorithm Using SIFT Feature

Our proposed ground target localization system is made up of two steps (shown in Figure 2).

As is shown in Figure 2, in the first step, SIFT descriptors are matched from UAV images and coarse positioning results, and location points are extracted from UAV images; in the second step, coordinate in coarse po-

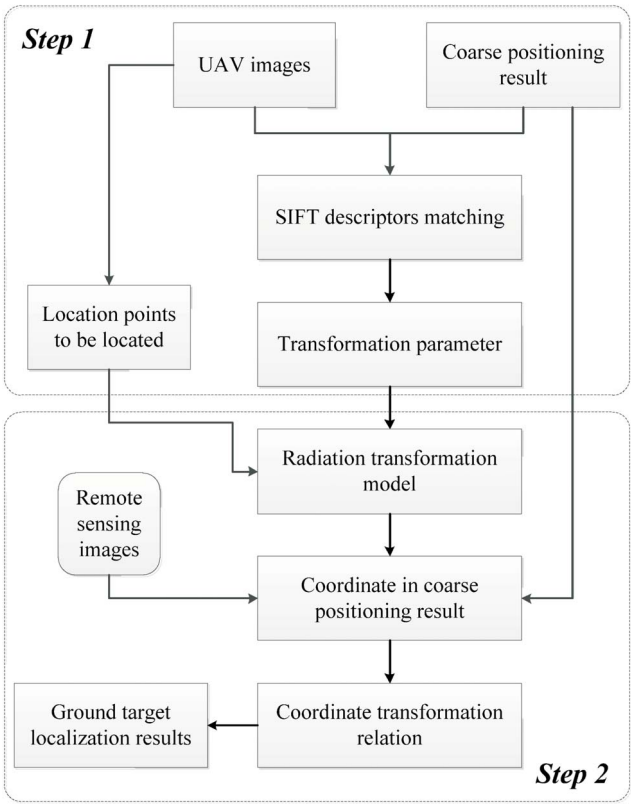

Figure 2. The proposed ground target localization system.

sitioning result is obtained from remote sensing images utilizing the radiation transformation model, and the final ground target localization results are gained from the coordinate transformation relation.

Feature matching refers to seek relationships between different image feature points after extracting visual features.

For the SIFT feature, we construct a feature vector and the match feature point by similarity calculation. Suppose that there are two feature vectors, that is $V_1 = (a_1, a_2, a_3, \ldots, a_n)$ and $V_2 = (b_1, b_2, b_3, \ldots, b_n)$. The distance between V_1 and V_2 is calculated as follows [19].

$$Dis = (V_1, V_2) = \arccos\left(\sum_{i=1}^{n}(a_i + b_i)\right) \tag{8}$$

where $i \in (1, 2, \ldots, n)$, and n denotes the number of dimension of feature vector.

As there are non-overlapping regions in images, feature points in these regions cannot be matched. However, SIFT feature matching algorithm still tries to find a feature point, and the matching results are obviously wrong. Therefore, in this paper, we exploit the Mahalanobis distance to re-match feature points. For a sample space with n points $Z = \{(x_1, y_1), (x_2, y_2), \ldots, (x_n, y_n)\}$. The Mahalanobis distance between sample $z_i = (x_i, y_i)$ and sample mean value $\mu = (\mu_x, \mu_y)$ is defined as follows.

$$MD_i = \sqrt{(z_i - \mu)^T C_z^{-1} (z_i - \mu)} \tag{9}$$

where C_z refers to the covariance matrix, μ means the sample mean value. The definition of C_z and μ are defined as follows.

$$C_z = \frac{1}{n} \cdot \left(\sum_{i=1}^{n} \begin{pmatrix} x_i - \mu_x \\ y_i - \mu_x \end{pmatrix} (x_i - \mu_x, y_i - \mu_x) \right) \tag{10}$$

$$\mu = [\mu_x, \mu_y] = \frac{1}{n} \left[\sum_{i=1}^{n} x_i, \sum_{i=1}^{n} y_i \right] \tag{11}$$

where [ ] refers to an expectation of the two random variables

The affine transformation denotes a function between affine spaces which preserves points, straight lines and planes. In particular, an affine transformation does not require preserve angles between lines or distances among points. Affine transformation model of this work is described as follows.

$$\begin{pmatrix} x_2 \\ y_2 \end{pmatrix} = s \cdot \begin{pmatrix} \cos\theta & -\sin\theta \\ \sin\theta & \cos\theta \end{pmatrix} \begin{pmatrix} x_1 \\ y_1 \end{pmatrix} + \begin{pmatrix} t_x \\ t_y \end{pmatrix} \tag{12}$$

where t_x and t_y denote translation, θ is the rotating angle, and s refers to a zoom scale. Moreover, (x_2, y_2) and (x_1, y_1) denote matching feature point pairs of image to be matched and the reference image.

More generally, 2D affine transformation is defined as follows.

$$\begin{pmatrix} x_2 \\ y_2 \end{pmatrix} = \left(\begin{pmatrix} a_{11} & a_{12} \\ a_{21} & a_{22} \end{pmatrix} \begin{pmatrix} x_1 \\ y_1 \end{pmatrix} \right) + \begin{pmatrix} a_{13} \\ a_{21} \end{pmatrix} \tag{13}$$

4. Experiment

In this section, we choose six UAV images to test the performance of the proposed algorithm. In 2D affine

transformation (show in Eq. 13), parameters are illustrated in Table 1.

Afterwards, in order to facilitate comparison, we normalize the range of X and Y coordinate to $0 \le X, Y \le 1$, and the target localization results of the above six images in the normalized range are shown in Figure 3 to Figure 8.

Integrating the above results, the average distances between actual data and the target localization results are given in Table 2 as follows.

In order to make performance comparison, we choose the deformable mesh registration based method (denoted as DMR) [17] to compare the accuracy of target localization of ours method. Experimental result is shown in Figure 9 as follows.

Figure 9 shows that the proposed method can achieve lower average distance in target localization than DMR.

To clearly describe the accuracy of the proposed algorithm, an example of target localization result is shown in Figure 10.

Based on all the above experimental results, it can be observed that the proposed algorithm is able to accurately detect and locate ground target in UAV images.

Table 1. Parameter of 2D affine transformation

Parameter	a_{11}	a_{12}	a_{21}	a_{22}	a_{13}
UAV image 1	0.9892	0.0037	0.0491	0.9975	0.2556
UAV image 2	-0.5396	-0.1852	1.1125	1.1152	3.7842
UAV image 3	0.9677	0.0074	0.0225	1.0023	6.2549
UAV image 4	-0.4458	-0.1597	1.0254	1.2478	3.6985
UAV image 5	0.9587	0.0147	0.0274	1.0147	5.9687
UAV image 6	0.9741	0.0052	0.0488	0.9834	0.2368

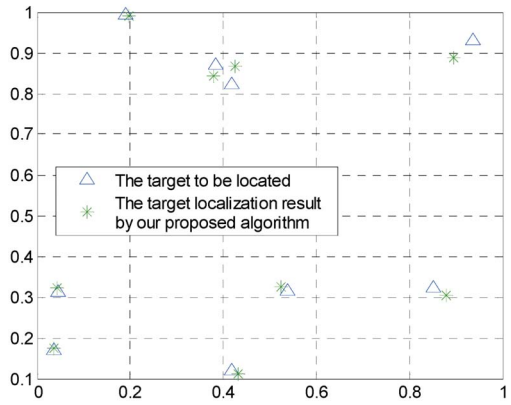

Figure 3. Target localization result in the normalized range (image 1).

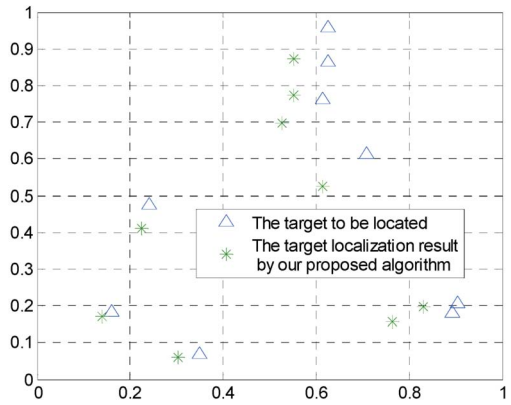

Figure 4. Target localization result in the normalized range (image 2).

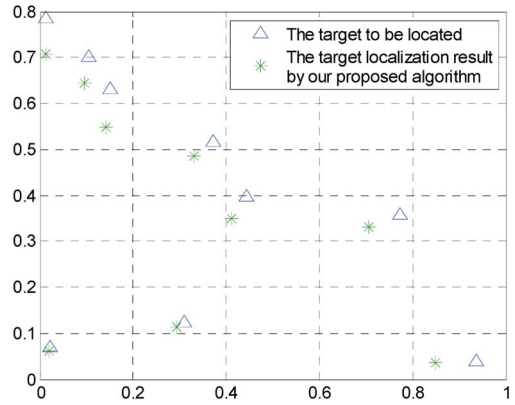

Figure 5. Target localization result in the normalized range (image 3).

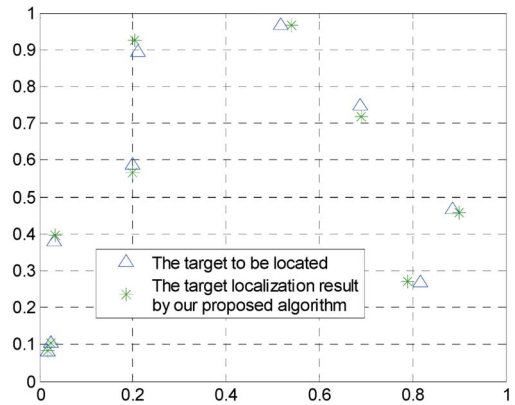

Figure 6. Target localization result in the normalized range (image 4).

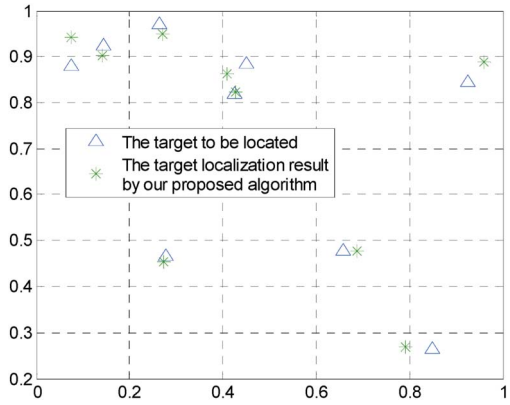

Figure 7. Target localization result in the normalized range (image 5).

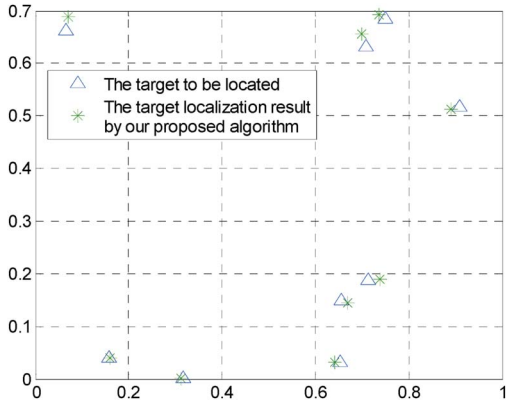

Figure 8. Target localization result in the normalized range (image 6).

Table 2. Average distance between actual data and the target localization results (Meter)

Image ID	Image 1	Image 2	Image 3	Image 4	Image 5	Image 6
Average distance	0.0244	0.0903	0.0563	0.0184	0.0369	0.0524
Standard deviation	0.0175	0.0358	0.0262	0.0254	0.0348	0.0391

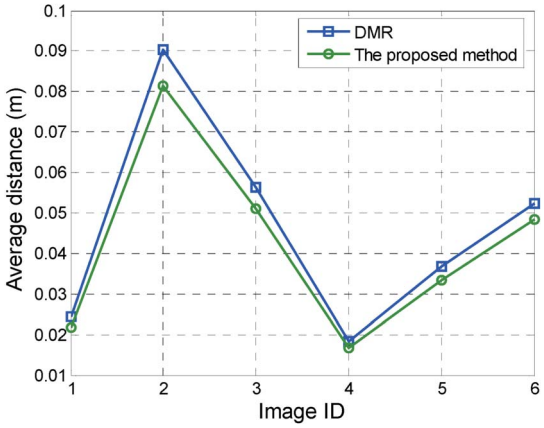

Figure 9. Performance comparison.

Figure 10. An example of target localization result.

5. Conclusion

This paper focuses on the problem of ground target localization from UAV images. SIFT features are used to describe visual contents of the UAV images. Main contributions of this paper lie in that 1) SIFT descriptors are matched from UAV images and coarse positioning result, and location points are extracted from UAV images, and 2) Coordinates in coarse positioning results are computed from remote sensing images using the radiation transformation model, and the ground target localization is found from the coordinate transformation relation. Experimental results show very positive results.

References

[1] Jabbari, A. H., and J. W. Yoon (2016) Robust Image-based Control of the Quadrotor Unmanned Aerial Vehicle, *Nonlinear Dynamics* 85(3), 2035–2048. doi: 10.1007/s11071-016-2813-2

[2] Eugene, M. (2016) Fractal Methods for Extracting Artificial Objects from the Unmanned Aerial Vehicle Images, *Journal of Applied Remote Sensing* 10, AR 025020. doi: 10.1117/1.JRS.10.025020

[3] Yang, Y., Z. J. Lin, and F. Z. Liu (2016) Stable Imaging

and Accuracy Issues of Low-altitude Unmanned Aerial Vehicle Photogrammetry Systems, *Remote Sensing* 8(4), AR 316. doi: 10.3390/rs8040316

[4] Abdulla, A. R., F. N. He, M. Adel, E. S. Naser, and H. Ayman (2016) Using an Unmanned Aerial Vehicle-based Digital Imaging System to Derive a 3D Point Cloud for Landslide Scarp Recognition, *Remote Sensing* 8(2), AR 95. doi: 10.3390/rs8020095

[5] Liu, S. J., X. H. Tong, J. Chen, X. F. Liu, W. Z. Sun, H. Xie, P. Chen, Y. M. Jin, and Z. Ye (2016) A Linear Feature-based Approach for the Registration of Unmanned Aerial Vehicle Remotely-sensed Images and Airborne LiDAR Data, *Remote Sensing* 8(2), AR 82. doi: 10.3390/rs8020082

[6] Xiao, X. W., B. X. Guo, D. R. Li, L. H. Li, N. Yang, J. C. Liu, P. Zhang, and Z. Peng (2016) Multi-view Stereo Matching Based on Self-adaptive Patch and Image Grouping for Multiple Unmanned Aerial Vehicle Imagery, *Remote Sensing* 8(2), AR 89. doi: 10.3390/rs8020089

[7] Flavia, T., P. Christopher, P. Paul, G. Salvatore, and P. Maurizio (2015) Large-scale Particle Image Velocimetry from an Unmanned Aerial Vehicle, *IEEE-ASME Transactions on Mechatronics* 20(6), 3269–3275. doi: 10.1109/TMECH.2015.2408112

[8] Feng, H. Z., H. W. Liu, J. K. Yan, F. Z. Dai, and M. Fang (2016) A Fast Efficient Power Allocation Algorithm for Target Localization in Cognitive Distributed Multiple Radar Systems, *Signal Processing* 127, 100–116. doi: 10.1016/j.sigpro.2015.12.022

[9] Chu, Y. L., L. Y. He, and F. Yao (2016) An Improved Localization Algorithm of Taylor Series Expansion Search Target, *OPTIK* 127(19), 8070–8075.

[10] Sajjad, B., Z. G. Sevgi, and U. B. Elif (2015) Implementation of an Enhanced Target Localization and Identification Algorithm on a Magnetic WSN, *IEICE Transactions on Communications* E98B(10), 2022–2032. doi: 10.1587/transcom.E98.B.2022

[11] Martin, E. and H. C. So (2015) Weighted Least Squares Algorithm for Target Localization in Distributed MIMO Radar, *Signal Processing* 115, 144–150.

[12] Joshua, V. H., T. Pratap, and I. Volkan (2015) Algorithms for Cooperative Active Localization of Static Targets with Mobile Bearing Sensors under Communication Constraints, *IEEE Transactions on Robotics* 31(4), 864–876. doi: 10.1109/TRO.2015.2432612

[13] Yacine, M., M. Said, F. Mouloud, Z. Abdelhalim, and A. Mehdi (2015) SV-training and Kernel Change Detection Algorithm for the Abrupt Modification in EMI Data for Buried Metallic Target Localization and Identification, *Applied Computational Electromagnetics Society Journal* 30(1), 132–139.

[14] Jang, E. J. and D. S. Han (2014) Location Adaptive Least Square Algorithm for Target Localization in Multi-static Active Sonar, *IEICE Transactions on Communications* E97B(1), 204–209. doi: 10.1587/transcom.E97.B.204

[15] Nikhil, D., G. Edward, and T. C. Henderson (2014) Target Localization and Autonomous Navigation Using Wireless Sensor Networks-A Pseudogradient Algorithm Approach, *IEEE Systems Journal* 8(1), 93–103. doi: 10.1109/JSYST.2013.2260631

[16] Damian, F., S. J. Walmsley, G. Anne-Claude, H. W. Choi, and A. I. Nesvizhskii (2013) LuciPHOr: Algorithm for Phosphorylation Site Localization with False Localization Rate Estimation Using Modified Target-decoy Approach, *Molecular & Cellular Proteomics* 12(11), 3409–3419. doi: 10.1074/mcp.M113.028928

[17] Scott, R., W. Elisabeth, and G. D. Hugo (2013) Deformable Mesh Registration for the Validation of Automatic Target Localization Algorithms, *Medical Physics*, 40(7), AR 071721. doi: 10.1118/1.4811105

[18] Huang, F. C., S. Y. Huang, J. W. Ker, and Y. C. Chen (2012) High-performance SIFT Hardware Accelerator for Real-time Image Feature Extraction, *IEEE Transactions on Circuits and Systems for Video Technology* 22(3), 340–351. doi: 10.1109/TCSVT.2011.2162760

[19] Fu, W. P., C. Qin, J. Liu, S. Q. Yang, and W. Wang (2011) Matching and Location of Image Object Based on SIFT Algorithm, *Chinese Journal of Scientific Instrument* 32(1), 163–169.

[20] Lowe, D. G. (2004) Distinctive Image Features from Scale-invariant Keypoints, *International Journal of Computer Vision* 60(2), 91–110. doi: 10.1023/B:VISI.0000029664.99615.94

Manuscript Received: May 4, 2017
Accepted: May 16, 2018